Binding of Adenosine Diphosphoribosyltransferase to the Termini and Internal Regions of Linear DNAs†

Srinivas S. Sastry,‡ Kalman G. Buki,§ and Ernest Kun*
Department of Pharmacology and the Cardiovascular Research Institute, University of California at San Francisco, San Francisco, California 94143

Received October 21, 1988; Revised Manuscript Received February 23, 1989

ABSTRACT: Binding mechanisms of ADPR-transferase to restricted double-stranded DNA fragments of SV40 and *pBR*322 DNA were determined by nuclease protection techniques. Top and bottom strands of double-stranded DNA were identified by specific labeling with ^{32}P. Protection against specific exonucleases identified binding of ADPR-transferase to DNA termini, whereas binding to internal regions of linear DNAs was probed by protection against endonucleases. ADPR-transferase protein protected against exonucleolytic attack from λ *exo* and *exo*III in all DNA fragments tested, demonstrating that the enzyme protein binds indiscriminately to all DNA termini. Extending earlier results [Sastry, S. S., & Kun, E. (1988) *J. Biol. Chem. 263*, 1505–1512], the modifying effect of the binding of ADPR-transferase to DNA induced changes in DNA conformation, as evident from altered pause sites that appeared following digestion of DNA fragments by λ exonuclease in the presence of ADPR-transferase. In contrast to the nonselective binding of ADPR-transferase to DNA termini, ADPR-transferase conferred protection against endonuclease attack (DNase I and micrococcal nuclease) only to the 209-bp *Eco*RI–*Pst*I SV40 DNA fragment. These results indicate that binding of ADPR-transferase to relatively rare internal regions of restricted DNA fragments exhibits some degree of specificity. Specificity of binding appears to be related to the coincidental relative A+T-rich regions in DNA, and to DNA bending, both identified in the 209-bp SV40 DNA fragment. Synthetic polydeoxyribonucleotides containing dA-dT bind ADPR-transferase stronger than polydeoxyribonucleotides containing dG-dC. It was deduced from endonuclease protection patterns that binding of the enzyme protein leaves no defined footprints on the 209-bp SV40 DNA fragment, but there is significant modification of DNA structure following binding of the enzyme protein. Methylation protection assays and the prevention of the binding of ADPR-transferase to T4 DNA by its glucosylation indicate that the enzyme binds in the major groove of DNA. The 36-kDa A peptide fragment of ADPR-transferase [Buki, K. G., & Kun, E. (1988) *Biochemistry 27*, 5990–5995] exhibits the same protection against endonucleolytic enzymes as the intact ADPR-transferase molecule.

Adenosine diphosphoribosyltransferase [ADPRT; poly(ADP-ribose) polymerase, EC 2.4.2.30] is a specific nuclear protein of higher eucaryotes that has been known primarily as a DNA-dependent enzyme (Kun et al., 1983a; Ueda & Hayaishi, 1985; Althaus & Richter, 1987) catalyzing the polymerization of ADP-R derived from NAD^+ to helical homopolymers (Minaga & Kun, 1983a,b) that are covalently bound to ADPRT and certain other nuclear proteins [cf. Althaus and Richter (1987)]. We have recently described a second molecular activity of this enzyme that is only secondarily regulated by the metabolic substrate of ADPRT, which is NAD^+, and consists of DNA condensation following the binding of ADPRT to certain circular double-stranded DNAs (e.g., SV40 DNA), an activity that is cooperative with histones (Sastry & Kun, 1988). Specific regions of circular SV40 DNA, when restricted, also bind ADPRT (Sastry & Kun, 1988), but there is selectivity with respect to the nature of the linearized double-stranded DNA ligands. It is known (Benjamin & Gill, 1980a,b) that the coenzymatic function of DNA, consisting of the augmentation of the enzyme-catalyzed poly(ADP-ribose) formation, is greatly increased following nuclease or chemically induced single- and double-stranded cuts of circular DNAs [cf. Gaal and Pearson (1985) and Althaus and Richter (1987)]. This implies that ADPRT binding to DNA termini may have primarily metabolic catalytic significance, whereas the recently described topological effect of ADPRT on DNA (Sastry & Kun, 1988), which does not involve DNA termini, serves a different purpose. The two types of ADPRT–DNA associations that probably have distinct cell biological significance require further experimental characterization. In the present paper we identify the binding of ADPRT to DNA termini with the aid of specific exonucleases by methods that have been tested in other systems (Riley & Wientraub, 1978; Von der Ahe et al., 1985; Slater et al., 1985; Shalloway et al., 1980; Wu, 1985; Elbrecht et al., 1985). On the other hand, the binding of ADPRT to internal regions of certain restricted double-strand DNAs proved to be more discriminating because it depended on the nature of the restricted DNA fragments. The binding of ADPRT to internal regions of restricted DNAs was determined by known methods that are based on the modification of the action of specific endonucleases on DNA (Galas & Schmitz, 1978). This procedure can identify the binding of proteins to specific DNA sequences that result in DNaseI "footprints", but if ADPRT binding regions with varying affinities exist in DNA, the interpretation of results tends to be more complicated. The binding of ADPRT to DNAs did not produce specific footprints, according to known criteria (Galas & Schmitz, 1978; Hochschild et al., 1986; Dynan & Tjian, 1983; Dynan et al.,

† This research was supported by Grants HL-27317 (NIH) and AFO-SR-85-0377 and AFO-SR-86-0064 (Air Force Office of Scientific Research). E.K. is a recipient of the Research Career Award of USPHS.

* To whom corrspondence should be addressed at Laboratory of Environmental Toxicology, San Francisco State University, Tiburon Center, 3150 Paradise Drive, Tiburon, CA 94920.

‡ Present address: Department of Chemistry, Hildebrand Hall, University of California, Berkeley, CA 94720.

§ Present address: Department of Biochemistry (II), Semmelweis University, Budapest, Hungary.

0006-2960/89/0428-5670$01.50/0

1986; Angel et al., 1988) that are consistent with a specific DNA sequence-restricted protein binding. However, one feature of DNA, that is, a bent structure, coincided with the ability of DNA to bind ADPRT. Furthermore, experiments with DNA methylation and the binding of ADPRT to non-glucosylated but not to glucosylated phage T4 DNA suggested major groove associations.

Materials and Methods

ADPRT, Nucleases, and DNA. ADPRT (M_r = 116000; 95% homogeneous) was purified from calf thymus as described elsewhere (Buki et al., 1987). DNase I and micrococcal nuclease were obtained from Cooper Biomedical (Malvern, PA). Exonuclease III and λ exonuclease were purchased from Bethesda Research Laboratories (Gaithersburg, MD). Restriction endonucleases were from New England Biolabs (Beverley, MA). T4 polynucleotide kinase, Klenow fragment, T4 and *Escherichia coli* DNA polymerases, terminal transferase from calf, and bacterial alkaline phosphatase were obtained from Boehringer Mannheim (Indianapolis, IN). [γ-^{32}P]ATP, [α-^{32}P]dATP, and [α-^{32}P]ddATP were from either Amersham Corp. (Arlington Heights, IL) or New England Nuclear (Boston, MA). SV40 DNA was purchased from Bethesda Research Laboratories. Plasmid *pBR*322 was prepared in the laboratory or obtained from Promega Biotech (Madison, WI). Plasmid *pSV*07 (containing the *Eco*RII G fragment of SV40 DNA) was a gift from Dr. Robert Tjian (University of California at Berkeley, Berkeley, CA), and phage T4 DNA was a gift of Dr. Bruce Alberts (University of California at San Francisco, San Francisco, CA). Poly(dI-dC)·poly(dI-dC) (average length = 500 bp), poly(dA-dT)·poly(dA-dT) (average length = 300 bp), and poly(dG-dC)·poly(dG-dC) (average length = 300 bp) were purchased from Pharmacia (Piscataway, NJ).

DNA Fragments. Fragment 1. This is a 209-bp *Eco*RI–*Pst*I fragment of SV40 DNA from position 1783 to position 1992 of the SV40 DNA (Buchman et al., 1980). This fragment lies within the coding region of VP1 (a viral coat protein) and has an overall A+T content of 60.2%, consisting of several contiguous runs of A+T residues (3–10 bp each) interspersed with not more than four consecutive G+C bp runs (see Figure 10A,E).

Fragment 2. This is a 154-bp *Acc*I–*Eco*RI piece of SV40 (between nucleotide positions 1628 and 1783; see Figure 10A) that contains a total of 54.5% A+T, however, only 3–9 bp A+T stretches and these are separated by nine blocks of G+C (3–5 bp each).

Fragment 3. This is a 311-bp *Eco*RII G DNA excised from *pSV*07 (between nucleotide positions 5092 and 160; see Figure 10A) containing the SV40 early transcriptional regulatory elements. This DNA has 48.8% A+T content that is dispersed as four maximally 17 bp A+T stretches in addition to 11 G+C segments (3–7 bp each).

Fragment 4. This is a 276-bp *Bam*HI–*Sal*I segment between nucleotide positions 375 and 651 of *pBR*322 as identified by Sutcliffe (1979) and has a 25.3% A+T content and not more than five contiguous A+T residues at any place. This linear DNA has several blocks of G+C (3–10 bp each), and the distribution of dA+dT and dG+dC approximates a mirror image of the 209-bp *Eco*RI–*Pst*I SV40 fragment with respect to dA+dT and dG+dC bases.

These DNAs were chosen for the nuclease protection experiments because of their suitable restriction sites and also because of the known differences in the distribution of A+T and G+C stretches within the fragments, which we postulated to be important in the specificity of ADPRT binding to DNA. The assignment of the positions of the nucleotides on the 209-bp *Eco*RI–*Pst*I fragment of SV40 DNA in the present work follows the numbering system employed by Buchman et al. (1980). For the 276-bp *Bam*HI–*Sal*I segment of *pBR*322, we adapted the numbering system of Sutcliffe (1979).

Preparation of DNA Fragments. SV40 DNA was first digested with *Eco*RI, and the 5′ ends were labeled with [γ-^{32}P]ATP and T4 polynucleotide kinase (see Figure 10B for a schematic diagram) or the 3′ ends labeled with [α-^{32}P]dATP and Klenow fragment (see Figure 10C). The linearized DNA was then digested with *Pst*I, and the resulting 209-bp fragment was purified from 5% nondenaturing polyacrylamide gels (Maniatis et al., 1982). The 3′ end of the *Pst*I site (see Figure 10D) of the 209-bp *Eco*RI–*Pst*I fragment was labeled with [α-^{32}P]ddATP and terminal nucleotidyltransferase (Roychaudhury & Wu, 1980). On the other hand, the 5′ end of the *Pst*I site, which consists of a 3′ overhang and recessed 5′ end, cannot be directly labeled with ^{32}P by customary methods (Maniatis et al., 1982) The 5′ ends of the *Eco*RI site or the 3′ ends of the *Pst*I site when labeled with T4 polynucleotide kinase and terminal nucleotidyltransferase, respectively, define the top strand, whereas labeling at the 3′ ends of the *Eco*RI site with Klenow fragment identifies the bottom strand, provided that redigestion of labeled strands with either *Pst*I or *Eco*RI is carried out subsequently, which leaves the 209-bp fragment labeled only at the 5′ or 3′ end, depending on the method of original labeling, thus identifying top and bottom strands directly (Maniatis et al., 1982). Uniquely end labeled fragments were prepared by digestion of SV40 DNA with *Acc*I–*Eco*RI, *Eco*RII G fragment from *pSV*07, and the digestion of *pBR*322 with *Bam*HI–*Sal*I.

Assay for the Protection by ADPRT against Exonuclease III and λ Exonuclease. Digestion with *exo*III was performed in a binding buffer (25 mM Tris-HCl, pH 8.0, 10 mM $MgCl_2$, 0.5 mM DTT, 0.1 M NaCl) as described for DNase I (see below). Five units of *exo*III were added to the initial binding mixture (50 μL), and the nuclease digestion was carried out in the presence or absence of ADPRT (see legend to Figure 2) for 30 min at 37 °C. Digestion with λ *exo* nuclease (10 units/50 μL test system at 37 °C for 20 min) and the initial binding of ADPRT were carried out in 67 mM glycine–KOH, pH 8.1, 2.5 mM $MgCl_2$, and 2.5 mM 2-mercaptoethanol because λ *exo* requires this buffer for maximal activity. *Exo*III and λ *exo* digestions were terminated as described for DNase I reactions.

Assay for Protection against DNase I by ADPRT. The technique of Galas and Schmitz (1978) was generally followed. The DNA fragments were mixed with purified ADPRT in the presence or absence of poly(dI-dC)·poly(dI-dC) (as competitor) in a final volume of 50 μL of binding buffer (see above) and incubated at 25 °C for 15 min. A freshly prepared solution of DNase I was added (0.5 units per 50-μL reaction) and further incubated with the ADPRT–DNA complex at 37 °C for 20–60 s, depending on the amount of ADPRT and/or synthetic polydeoxyribonucleotide competitors to yield comparable degrees of DNase I cleavage per test. The digestion was stopped by the addition of EDTA (10 mM final concentration) and SDS (0.1% final concentration), and samples were heated in a water bath at 90 °C for 3 min, precipitated with 0.3 M sodium acetate and EtOH, rinsed once with 70% EtOH, and redissolved in formamide-containing tracking dyes for electrophoresis on denaturing polyacrylamide gels (Maxam & Gilbert, 1980).

Assay for Protection by ADPRT against Micrococcal Nuclease. Micrococcal nuclease tests were similar to DNase I

assays except that after the initial binding of ADPRT to DNA at 25 °C for 15 min, $CaCl_2$ (to a final concentration of 2.5 mM) was added followed by micrococcal nuclease (1.5 units per 50-μL reaction). The reaction mixture was then incubated at 37 °C for 7–10 min and terminated as described for DNase I.

Assay for Protection by ADPRT against Methylation by Dimethyl Sulfate (DMS). The procedure of Siebenlist and Gilbert (1980) was generally followed. Approximately 200 ng (~1 × 10^5 cpm) of the ^{32}P-labeled 209-bp SV40 DNA fragment was mixed with ~2000 ng of ADPRT in 100 μL of methylation buffer (50 mM sodium cacodylate, pH 8.0, plus 10 mM $MgCl_2$ plus 0.1 mM EDTA plus 1.0 mM DTT plus 100 mM NaCl). The reaction mixture was incubated at 25 °C for 15 min. The protein–DNA complexes were then treated with 1 μL of a 10.5 M solution of dimethyl sulfate (Aldrich Chemical Co.) for 1 min at room temperature (22–25 °C). The volume of the solution was increased to 1 mL by the addition of 900 μL of binding buffer (see assay for the protection by ADPRT against exonuclease III and λ exonuclease, above). The solution was immediately filtered through nitrocellulose filters. The filter was washed once with 1 mL of binding buffer. The filtrate was collected, and the DNA in the filtrate was concentrated by EtOH precipitation. The filter-bound DNA was eluted off the filters as described in Sastry and Kun (1988). Both filter-bound and unbound (i.e., DNA that passed through the filter) DNAs were subsequently cleaved at modified dG residues as described by Siebenlist and Gilbert (1980) and Maxam and Gilbert (1980). The products of the cleavage reactions were separated on a denaturing polyacrylamide gel as described below. Methylation of naked 209-bp SV40 DNA by DMS did not per se increase or decrease the retention of labeled DNA fragments on nitrocellulose filters.

Separation of Nuclease Products by Gel Electrophoresis. The nuclease-digested DNA samples were resuspended in 7 μL of formamide-containing tracking dyes (80% v/v formamide, 0.02% w/v xylene cyanol, and 0.02% w/v bromophenol blue) and heated in a water bath at 90 °C for 3 min before loading on a 40 × 35 cm 10% acrylamide–7 M urea sequencing gel (Maxam & Gilbert, 1980). The gels were run at 1500 V until the bromophenol blue dye was about 6–8 cm from the bottom of the gel. Maxam–Gilbert chemical cleavage products were run alongside the nuclease-digested DNA samples as markers (Maxam & Gilbert, 1980). After the electrophoresis was completed, the gels were either dried or directly exposed to X-ray film (Kodak XOMAT AR-5) with or without an intensifying screen usually for 12–72 h. The positions of the nuclease cleavage sites were accurately identified at the nucleotide level when fragments were 50–70 bases long. In the case of DNA fragments longer than 70 bases, mapping of the nuclease cleavage sites may have an error of 1–2 bases.

Electrophoretic Assay for DNA Bending. The procedure was adopted from the method of Marini et al. (1982). The DNA fragments were separated in the cold (4 °C) at a constant voltage of 0.5 V/cm^2 in 1× Tris–borate EDTA buffer (Maniatis et al., 1982) on either 2% agarose gels or 5 or 12% polyacrylamide gels.

Detection of the DNA Binding of Polypeptides Prepared from ADPRT. Digestion of ADPRT with plasmin, polyacrylamide gel electrophoresis of the polypeptides, and electroblotting of the polypeptides onto nitrocellulose membranes were described previously (Buki et al., 1987). The nitrocellulose membranes with the polypeptides bound to them were washed for 2 h at room temperature (22 °C) in the binding buffer (see DNaseI Protection Assay) and then bathed overnight at room temperature in a solution of binding buffer, containing ^{32}P-labeled 209-bp *Eco*RI–*Pst*I fragment (~10^6 cpm) of SV40 (see Preparation of DNA Fragments), and subsequently washed with several changes of the binding buffer for 2 h at room temperature, air-dried at room temperature, and exposed overnight to X-ray film with an intensifying screen.

Results

Prevention of the Exonucleolytic Digestion of DNA by the Binding of ADPRT. Digestion by λ Exonuclease (5′→3′). Digestion with λ exonuclease of the 209-bp *Eco*RI–*Pst*I fragment of SV40 DNA, labeled with ^{32}P at the *Pst*I site identifying the top strand (see Materials and Methods and Figure 10D), proceeded to an extent of more than 90%, yielding DNA pieces with various length and with the λ *exo* activity showing several prominent pause sites (Figure 1A, lane 3). Binding of increasing amounts of ADPRT to the 209-bp fragment progressively inhibited the processive degradation by λ *exo* (Figure 1A, lanes 4–6) apparently from the 5′ end of the top strand. Some DNA degradation still occurred even at the highest concentration of ADPRT employed (Figure 1A, lane 5). Prominent λ *exo* pause sites on the top strand that were seen in the absence of ADPRT were abolished by ADPRT binding, consistent with a possible conformational change of DNA which takes place upon the binding of ADPRT. As a result of the binding of ADPRT, a new minor λ *exo* pause site emerges (at approximately position 1897, Figure 1A; ▼, Figure 10E), suggesting an ADPRT binding site at this particular DNA region of the top strand. Other regions that were associated with ADPRT were identified by several new pause sites. It is plausible to assume that, in a double-stranded DNA, ADPRT must make also contacts with the bottom strand, and this association may affect the binding of ADPRT to the top strand. This event could result in the appearance of a new λ *exo* pause site (at position ~1897) observed on the top strand. When the 3′ end of the *Eco*RI site was labeled with ^{32}P, results shown in Figure 1B illustrate that λ *exo* has only one (or a group of closely spaced unresolved) major pause site(s) on the bottom strand, unlike the top strand where several major pause sites appeared (compare lane 3, Figure 1A, with lane 2, Figure 1B). Binding of ADPRT abolished the pause site(s) (lanes 3 and 4, Figure 1A) and induced the appearance of a new pause site at approximately 1917 (lane 4, Figure 1B) as mapped on the bottom strand (▲, Figure 10E). The possibility that ADPRT molecules bound to the opposite strand may induce a new pause at position 1917 cannot be excluded. A possible inhibition of the λ *exo* activity by the binding of ADPRT to DNA was excluded by the addition of a 10-fold mass excess of unlabeled 209-bp SV40 fragment (lane 7, Figure 1A; lanes 5 and 6, Figure 1B), which restored the original exonuclease digestion pattern. this rules out a direct inhibitory action of ADPRT on λ *exo*.

Digestion with Exonuclease III. Binding of ADPRT to the 3′ end of the top strand (see Figure 10D) blocked the digestion of the DNA from the 3′ end (lanes 3 and 4, Figure 2A), and unlike digestion with λ *exo*, no small DNA fragments were generated by *exo*III. The differences between the two exonuclease digestion patterns of the DNA–ADPRT complexes cannot be attributed to phosphate groups of the 5′ end (versus a hydroxyl group on the 3′ end) because dephosphorylation at the 5′ ends did not change the results obtained with λ *exo* (data not shown). ADPRT has no direct inhibitory effect on

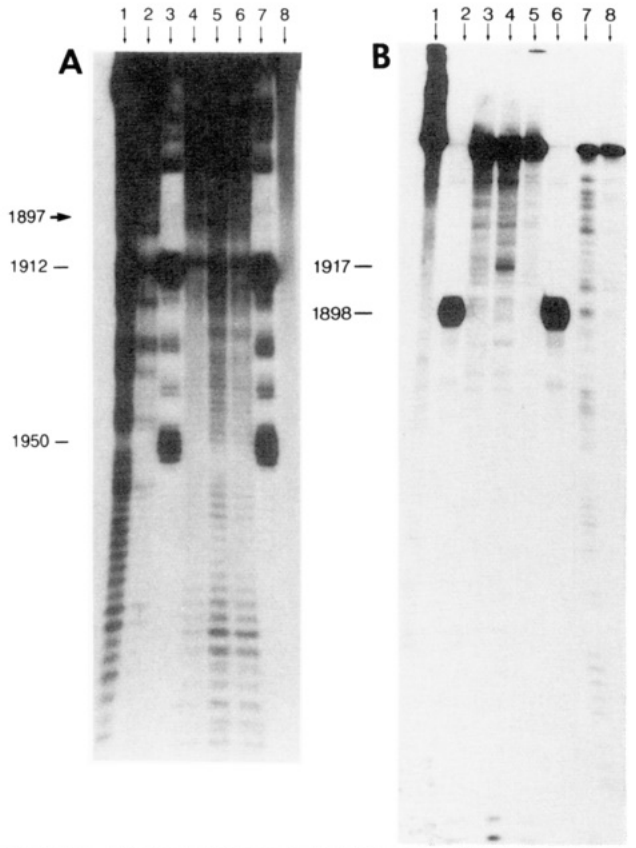

FIGURE 1: (A) λ exonuclease protection assay of ADPRT with the 209-bp *Eco*RI–*Pst*I SV40 DNA fragment ^{32}P-labeled at the 3′*Pst*I site: (lane 1) C+T markers; (lane 2) C markers; (lane 3) ^{32}P-labeled DNA digested in the absence of ADPRT; (lanes 4–6) ^{32}P-labeled DNA plus 100, 300, and 60 ng of ADPRT, respectively; (lane 7) ^{32}P-labeled DNA plus 300 ng of ADPRT plus 500 ng of unlabeled 209-bp *Eco*RI–*Pst*I SV40 DNA fragment; (lane 8) undigested ^{32}P-labeled DNA (a small amount of spontaneous degradation occurred during storage of the DNA because of the ^{32}P label, but no specific bands are seen). Each lane contained ~75 ng (5×10^4 cpm) of ^{32}P-labeled DNA fragment. The concentration of λ *exo* was 10 units per 50-μL test. (B) λ exonuclease protection assay of ADPRT with the 209-bp *Eco*RI–*Pst*I SV40 DNA fragment ^{32}P-labeled at the 3′*Eco*RI site: (lane 1) undigested ^{32}P-labeled DNA (a small amount of spontaneous degradation occurred during storage of the DNA because of the ^{32}P label, but no specific bands are seen); (lane 2) ^{32}P-labeled DNA digested in the absence of the ADPRT; (lanes 3 and 4) ^{32}P-labeled DNA plus 60 or 300 ng of ADPRT, respectively; (lane 5) ^{32}P-labeled DNA plus 300 ng of ADPRT plus 50 ng of unlabeled 209-bp *Eco*RI–*Pst*I SV40 DNA fragment; (lane 6) ^{32}P-labeled DNA plus 300 ng of ADPRT plus 500 ng of unlabeled 209-bp *Eco*RI–*Pst*I SV40 DNA fragment; (lane 7) C+T markers; (lane 8) C markers. Each lane contained ~50 ng (5×10^3 cpm) of ^{32}P-labeled DNA fragment. The concentration of λ *exo* was 10 units per 50-μL test.

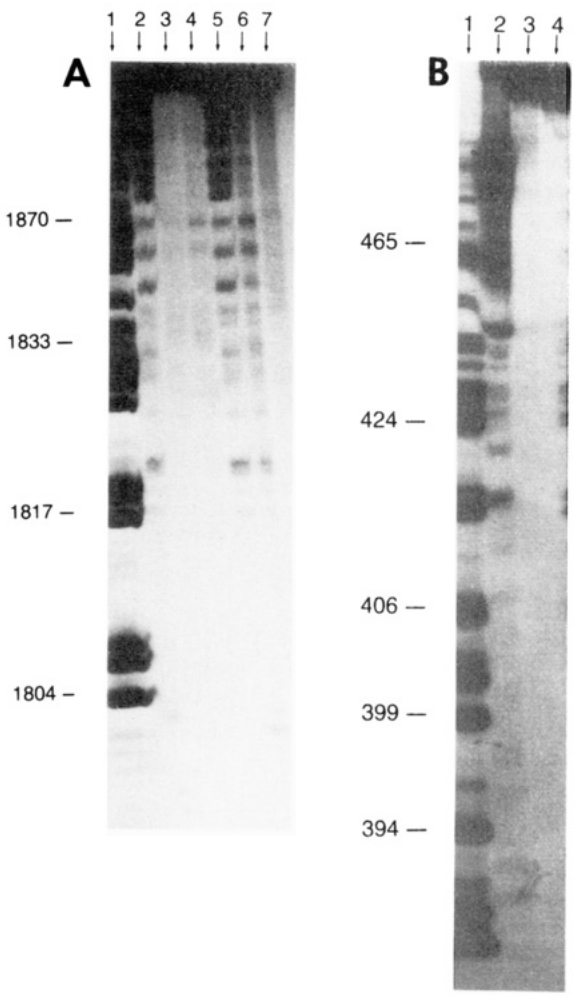

FIGURE 2: (A) Exonuclease III protection assay of ADPRT with the 209-bp *Eco*RI–*Pst*I SV40 DNA fragment ^{32}P-labeled at the 5′*Eco*RI site: (lane 1) G markers; (lane 2) ^{32}P-labeled DNA plus 300 ng of ADPRT plus 500 ng of unlabeled 209-bp *Eco*RI–*Pst*I SV40 DNA fragment; (lanes 3 and 4) ^{32}P-labeled DNA plus 300 or 60 ng of ADPRT, respectively; (lane 5) ^{32}P-labeled DNA digested in the absence of ADPRT; (lane 6) ^{32}P-labeled DNA plus 300 ng of ADPRT plus 1000 ng of poly(dI-dC)·poly(dI-dC) as a competitor; (lane 7) undigested ^{32}P-labeled DNA (a small amount of spontaneous degradation occurred during storage of the DNA because of the ^{32}P label, but no specific bands are seen). Each lane contained ~75 ng (5×10^4 cpm) of ^{32}P-labeled DNA fragment. The concentration of *exo*III was 5 units per 50-μL test. (B) Exonuclease III protection assay of ADPRT with the *Bam*HI–*Sal*I fragment of *pBR*322 ^{32}P-labeled at the 5′*Bam*HI site: (lane 1) G markers; (lane 2) ^{32}P-labeled DNA digested in the absence of ADPRT; (lanes 3 and 4) ^{32}P-labeled DNA plus 60 or 300 ng of ADPRT, respectively. Each lane contained ~50 ng (5×10^3 cpm) of ^{32}P-labeled DNA fragment. The concentration of *exo*III was 5 units per 50-μL test.

*exo*III (lane 2, Figure 2A). Poly(dI-dC)·poly(dI-dC) competes for ADPRT binding to the 3′ ends (lane 6, Figure 2A). It may be sufficient for ADPRT to bind to only one end of the two strands (either 5′ or 3′) and still restrict access of the nuclease to the free end of the opposite strand.

Several restriction fragments other than the 209-bp fragment were also tested in the λ *exo* and *exo*III assays, and competition with various polydeoxyribonucleotides was determined. Results were generally the same as with the 209-bp *Eco*RI–*Pst*I fragment of SV40 DNA. ADPRT was bound to the 3′ end of the top strand of the *Bam*HI–*Sal*I fragment of *pBR*322 (Figure 2B) and to the 5′ ends of the *Bam*HI–*Sal*I fragment of *pBR*322 as tested with the λ *exo* assay (results not shown). Polynucleotides such as poly(dI-dC)·poly(dI-dC) and poly(dA-dT)·poly(dA-dT) also bound ADPRT at the 5′ and 3′ ends. These experiments demonstrate that ADPRT binds to the termini (5′ and 3′) of linear DNAs in a nonselective manner.

Modification of the Effect of DNase I on the 209-bp DNA by ADPRT. Figure 3 shows the DNase I digestion pattern from the *Eco*RI end with the top strand labeled and the effect of ADPRT binding to the 209-bp *Eco*RI–*Pst*I fragment of SV40 DNA. At lower concentrations of ADPRT (lanes 3–5, Figure 3) several DNase I sites (arrows in Figure 3) were protected by ADPRT, and protection was proportional to ADPRT concentration (lanes 3–6, Figure 3). The bottom strand from the *Eco*RI end (Figure 4, lanes 4 and 5) revealed a small region of protection by low concentrations of ADPRT (position ~1820–1825) and a few additional protected sites (arrows on the bottom strand between positions 1796 and 1802, and at 1807, Figures 4 and 10E). Certain cutting sites of

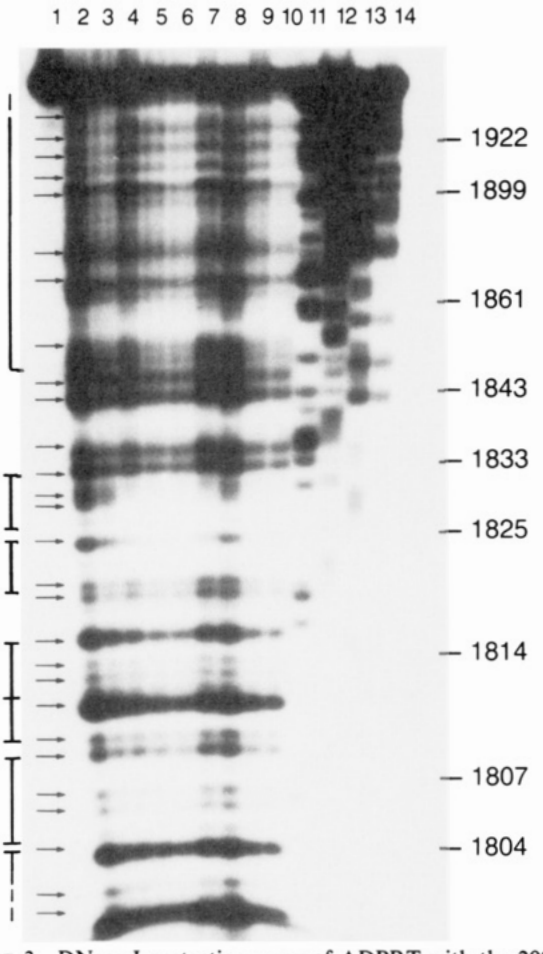

FIGURE 3: DNase I protection assay of ADPRT with the 209-bp *Eco*RI–*Pst*I SV40 DNA fragment ^{32}P-labeled at the 5′*Eco*RI site: (lane 1) undigested ^{32}P-labeled DNA; (lane 2) ^{32}P-labeled DNA digested for 30 s in the absence of the ADPRT; (lanes 3–6) ^{32}P-labeled DNA plus 60, 25, 100, or 500 ng of ADPRT, respectively; (lanes 7 and 8) ^{32}P-labeled DNA plus 1000 or 5000 ng of poly(dI-dC)·poly(dI-dC), respectively, plus 500 ng of ADPRT at each concentration of the competitor polynucleotide; (lanes 9 and 10) ^{32}P-labeled DNA plus 100 or 500 ng of 36-kDa A polypeptide, respectively; (lanes 11–14) G, G+A, C, and C+T markers, respectively. The concentration of DNase I was 0.5 units per 50-μL reaction. The markers toward the bottom of the gel are faint due to photographic reproduction, but they could be seen clearly on the original autoradiogram. Each lane contained ~50 ng (5×10^4 cpm) of ^{32}P-labeled DNA. Arrows show examples of several sites where DNase I cleavage is suppressed in the presence of ADPRT or the 36-kDa A polypeptide. The brackets denote regions of ADPRT or the 36-kDa A polypeptide binding. The brackets are drawn in an arbitrary manner to show binding regions falling between the most prominent DNase I cutting sites. The hyphenated lines at the bottom and the top of the gel signify the lack of definition at the ends of the DNase I protected regions.

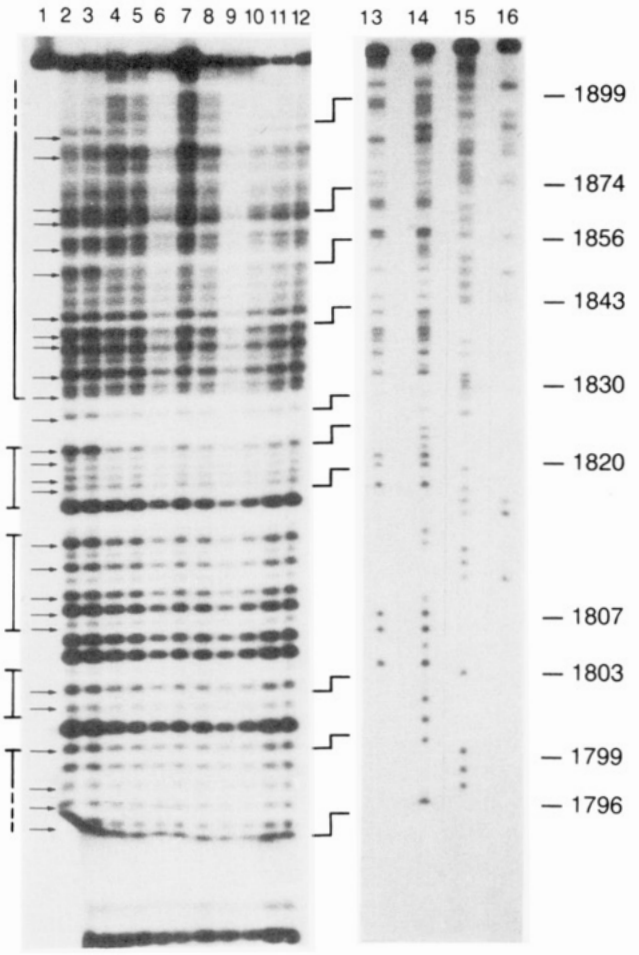

FIGURE 4: DNase I protection assay of ADPRT with the 209-bp *Eco*RI–*Pst*I SV40 DNA fragment ^{32}P-labeled at the 3′*Eco*RI site: (lane 1) undigested ^{32}P-labeled DNA; (lanes 2 and 3) ^{32}P-labeled DNA digested for 30 or 20 s, respectively, in the absence of ADPRT; (lanes 4–6) ^{32}P-labeled DNA plus 60, 100, or 500 ng of ADPRT, respectively; (lanes 7 and 8) ^{32}P-labeled DNA plus 1000 or 5000 ng of poly(dI-dC)·poly(dI-dC), respectively, plus 300 ng of ADPRT at each concentration of the competitor polynucleotide; (lanes 9–11) ^{32}P-labeled DNA plus 500, 100, or 60 ng of 36-kDa A polypeptide, respectively; (lane 12) ^{32}P-labeled DNA plus 5000 ng of poly(dI-dC)·poly(dI-dC) plus 500 ng of 36-kDa A polypeptide; (lanes 13–16) C, C+T, G+A, and G markers, respectively. Each lane contained ~50 ng (2×10^4 cpm) of ^{32}P-labeled DNA. The concentration of DNase I was 0.5 units per 50-μL reaction. All the lanes in the figure are from the same gel, but the markers were loaded several lanes away from the experimental samples. Due to expansion of the wells at the outside portions of the gel during preelectrophoresis and electrophoresis, there was a slight artifact in their migration; therefore, lines have been drawn in the middle of the photograph to show the correspondence (which was known from other gels of the same experimental protocol) between the experimental samples and the markers. Arrows show examples of several sites of suppressed DNase I cleavage in the presence of ADPRT or the 36-kDa A polypeptide. The brackets denote regions of ADPRT or the 36-kDa A polypeptide binding. The brackets are drawn in an arbitrary manner to show binding regions falling between the most prominent DNase I cutting sites. The hyphenated lines at the bottom and the top of the gel signify the lack of definition at the ends of the DNase I protected regions.

DNase I were actually enhanced by ADPRT binding (positions ~1899–~1923, lanes 4 and 5, Figure 4) as compared to the effect of DNase I on naked DNA (positions ~1899–~1923, lanes 2 and 3, Figure 4). At the highest concentration of ADPRT, large protected regions were only observed on the bottom strand (Figure 4, lane 6; Figure 10E, ~1831–1922), and there was a sharp decrease in the overall cutting frequency at all DNase I sites (Figure 4, lane 6). At the highest concentration of ADPRT DNase I protection on the top strand (Figure 3) roughly overlapped that on the bottom strand (Figure 10E), whereas at low concentrations of ADPRT a distinction between the two strands was apparent. For example, between position 1843 and the top of the gel (compare lanes 2 and 5 in Figure 3) clear protection by low concentration of ADPRT is visible on the top strand but not on the bottom strand (lane 5, Figure 4, position 1843 to the upper end of the gel). ADPRT binding does not shift the DNase I cutting sites, only competes with the endonuclease for the same DNase I sites (Figures 3 and 4), and no distinct boundaries of the protected regions can be defined, as indicated by the dashed lines (Figures 3, 4, and 10E).

In contrast to the relatively uncomplicated protection pattern by ADPRT against DNase I attack on the 209-bp DNA, labeled from the *Eco*RI end, results of DNase I digestion from

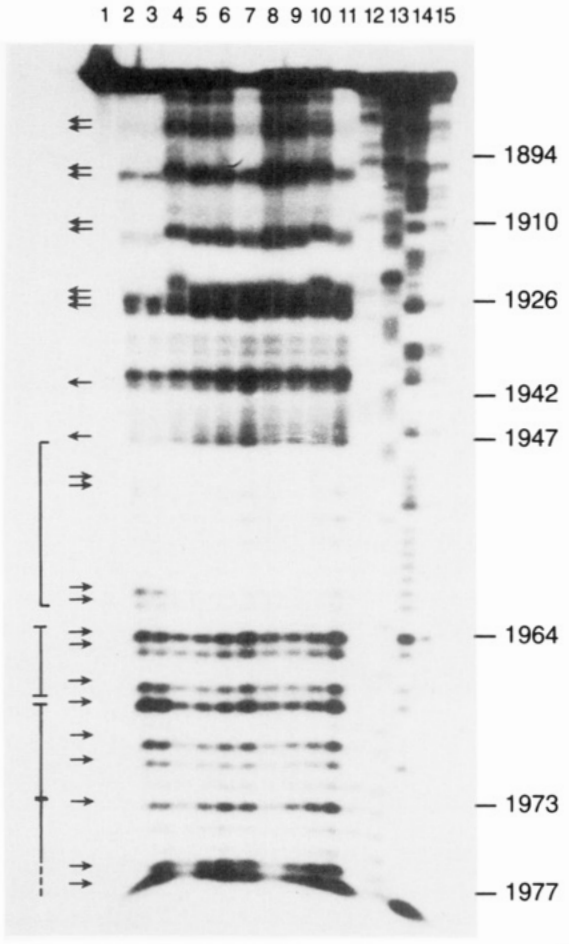

FIGURE 5: DNase I protection assay of ADPRT with the 209-bp *Eco*RI–*Pst*I SV40 DNA fragment ^{32}P-labeled at the 3′*Pst*I site: (lane 1) undigested ^{32}P-labeled DNA; (lanes 2 and 3) ^{32}P-labeled DNA digested for 20 or 30 s, respectively, in the absence of ADPRT; (lanes 4–6) ^{32}P-labeled DNA plus 500, 100, or 60 ng of ADPRT, respectively; (lane 7) ^{32}P-labeled DNA plus 5000 ng of poly(dI-dC)·poly(dI-dC) plus 500 ng of ADPRT; (lanes 8–10) ^{32}P-labeled DNA plus 500, 100, or 60 ng of 36-kDa A polypeptide, respectively; (lanes 12–15) G, G+A, C, and C+T markers, respectively. The concentration of DNase I was 0.5 units per 50-μL reaction. The markers toward the bottom of the gel are faint due to photographic reproduction, but they could be seen clearly on the original autoradiogram. Each lane contained ~50 ng (2×10^4 cpm) of ^{32}P-labeled DNA. Toward the top of the gel where the resolution of the bands decreases, each arrow does not necessarily indicate the presence of only one band but may signify multiple close sites. The significance of the arrows and the brackets is the same as explained in the legends to Figures 3 and 4. ⌐¬ indicates a region of low-frequency DNase I cutting. We have observed, only in the case the 209-bp SV40 fragment, that the products of nuclease digestion migrating at the top of a sequencing gel may have a tendency to form secondary structures and hence are sometimes poorly resolved. This phenomenon was seen even though the gels were run between 50 and 55 °C. However, the enhanced sites of DNase I cleavage are clearly visible.

the *Pst*I end (Figure 10D) yielded highly anomalous results, which could not be readily explained unless one assumed that there was a significant change in DNA conformation (Sastry & Kun, 1988) following the binding of ADPRT, which indirectly modified DNase I sites. The DNase I cleavage pattern following the binding of ADPRT (lanes 4–6, Figure 5) was either decreased (arrows pointing to the right-hand side, Figure 5) or enhanced (arrows pointing to the left-hand side, Figure 5) as compared to the cleavage of the naked DNA (lanes 2 and 3, Figure 5). At low concentrations of ADPRT (lanes 5 and 6, Figure 5), only a few protected sites and many enhanced sites are observed on the top strand from the *Pst*I end in contrast to the top strand from the *Eco*RI end (Figure 3), where only protected sites were present. The enhanced cleavage sites (~5–15-fold enhancement) and the suppressed sites for DNase I are shown in Figure 10E. At the highest concentration of ADPRT there were no large protected regions on the top strand from the *Pst*I end (Figure 5, land 4; position ~1863–1923 in Figure 10E) that corresponded to the protected region mapped on the top strand in Figure 3 from the *Eco*RI end. Enhanced sites shown in Figure 5 (lanes 4–6) between position ~1926 and the top of the gel (~1874) are not seen in Figure 3 (lanes 5 and 6). The protected sites illustrated in Figure 3 (lanes 5 and 6, position ~1922 to the top of the gel) are not present in Figure 5 (lanes 4–6). These seemingly contradictory digestion patterns between Figures 3 and 5 may be partly explained by the statistical distribution (Brenowitz et al., 1986) of DNase I generated fragments (~1874–1926) that were selectively labeled. Figure 5 indicates a relatively large region (positions 1947–1964, Figures 5 and 10E) of infrequent DNase I cutting sites, and ADPRT protected regions (|—|, Figure 10E) appear to be roughly equivalent to half a turn (5–6 bp) of helical B DNA. The nucleotide sequences that are protected overall against DNase I by ADPRT are shaded in Figure 10E.

Limitations of the electrophoretic technique curtailed an accurate determination of ADPRT binding to the *Eco*RI and *Pst*I ends of DNA, since smaller fragments than 5–13 bases could not be analyzed by the electrophoresis and thus were either not generated or remained undetected (Figures 3–5). Taking into account these uncertainties, our results suggest a relatively weak binding of DNase I to these DNA regions, a conclusion compatible with the crystallographic model of Suck and Oefner (1986).

Poly(dI-dC)·poly(dI-dC), a nonspecific polynucleotide that has been used as a competitor (Dynan & Tjian, 1983; Angel et al., 1988) in DNase I footprinting experiments, was also tested as an inhibitor of the formation of the ADPRT–209-bp DNA complexes. Poly(dI-dC)·poly(dI-dC) inhibited the binding of ADPRT to the 209-bp *Eco*RI–*Pst*I fragment at the DNase I protected regions (Figure 3, lanes 7 and 8; Figure 4, lanes 7 and 8; Figure 5, lane 7).

ADPRT did not protect three other DNA fragments (*Acc*I–*Eco*RI of SV40; the *Eco*RII G of SV40 DNA, whose positions are shown in Figure 10A; and the *Bam*HI–*Sal*I fragment of *pBR*322) against the endonucleolytic attack by DNase I (data not shown). We therefore conclude that the binding of ADPRT to internal regions of the 209-bp *Eco*RI–*Pst*I fragment is a relatively rare event and does not indicate an indiscriminate association of ADPRT to any internal region of double-stranded DNA.

Protection by ADPRT against Digestion of the 209-bp DNA by Micrococcal Nuclease. Digestion of protein–DNA complexes with micrococcal nuclease yields generally larger regions of protection than with DNase I as reported for DNA–DNA gyrase complexes (Lui & Wang, 1978; Morrison & Cozzarelli, 1981) and for nucleosomes (Noll, 1974). In the presence of low concentrations of ADPRT (60–200 ng of ADPRT plus ~50 ng of DNA per test) some prominent micrococcal nuclease cutting sites (approximately between positions 1789 and 1802) occurred in the 209-bp SV40 DNA fragment. At higher concentrations of ADPRT (300–500 ng of ADPRT plus ~50 ng of DNA per test), the size of the protected region widened, and at the highest concentration of ADPRT (1000 ng of ADPRT plus ~50 ng of DNA per test), the protected regions by ADPRT were entirely contiguous (data not shown) without discernible cutting sites, implying that ADPRT successfully competed for all binding sites of micrococcal nuclease. Mi-

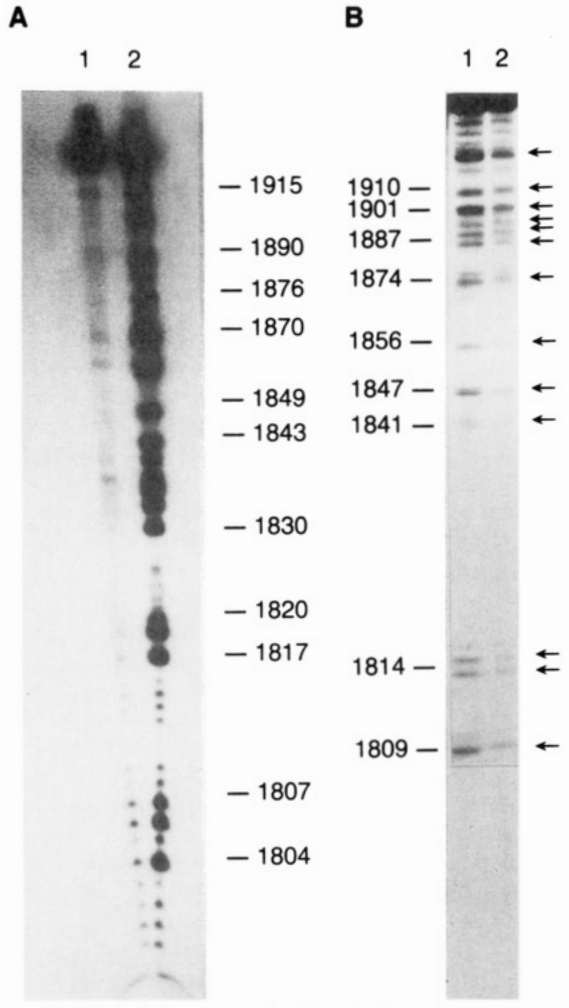

FIGURE 6: Methylation protection by ADPRT of the 209-bp *Eco*RI–*Pst*I SV40 DNA fragment ^{32}P-labeled at the 5′*Eco*RI site (A) or the 3′*Eco*RI site (B). (A) (Lane 1) Filter-bound ^{32}P-labeled DNA, i.e., DNA bound by ADPRT; (lane 2) ^{32}P-labeled DNA that passed through the nitrocellulose filter, i.e., ADPRT-free DNA. Each lane contained ~5 × 10^4 cpm. (B) (Lane 1) ^{32}P-labeled DNA that passed through the nitrocellulose filter, i.e., ADPRT-free DNA; (lane 2) filter-bound ^{32}P-labeled DNA, i.e., DNA bound by ADPRT. Each lane contained ~5 × 10^3 cpm. The arrows indicate dGs that are partially protected from methylation by DMS.

crococcal nuclease protection assays with fragments that were labeled at the 5′-*Eco*RI site (with ^{32}P) could not be performed because of the pronounced exonuclease (5′ phosphodiesterase) activity of the nuclease preparations.

Consistent with the relative selectivity of ADPRT binding to the 209-bp SV40 DNA fragment as determined by the DNase I protection assay, micrococcal nuclease digestion did not indicate binding of ADPRT to the *Bam*HI–*Sal*I fragment of *pBR*322 (data not shown).

Modification of the Effect of Dimethyl Sulfate (DMS) on the 209-bp DNA by the Binding of ADPRT. Experiments performed according to the nitrocellulose filter binding procedure of Siebenlist Gilbert (1980) showed (Figure 6A, lane 1) an almost complete absence of the methylation of dGs in the top strand following binding of ADPRT to DNA. On the other hand, with ADPRT-free DNA, dG residues were readily accessible to methylation by DMS (lane 2, Figure 6A). Several dG residues in the bottom strand were only moderately protected from methylation by ADPRT (compare lanes 2 and 1, Figure 6B). These results demonstrate that ADPRT makes major groove contacts and displays stronger affinity to the top strand than to the bottom strand of the 209-bp fragment.

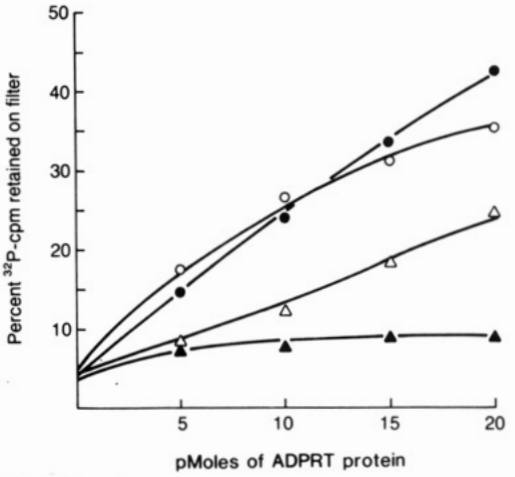

FIGURE 7: Binding of ADPRT to T4 DNA, poly(dA-dT)·poly(dA-dT), and poly(dG-dC)·poly(dG-dC): Increasing amounts of ADPRT were incubated with nick-translated (using either T4 DNA polymerase for T4 DNA or *E. coli* DNA polymerase for the polynucleotides) T4 DNA (HMdC or gluc HMdC),poly(dA-dT)·poly(dA-dT), and poly(dG-dC)·poly(dG-dC) [~20–50 ng (10^5 cpm) of each DNA] in 50 μL of binding buffer at 25 °C for 20 min. The reaction mixtures were then filtered through nitrocellulose disks, and the filter-bound ^{32}P cpm was counted in a scintillation counter as described in Sastry and Kun (1988). (○) Nonglucosylated T4 DNA; (▲) glucosylated T4 DNA; (●) poly(dA-dT)·poly(dA-dT); (△) poly(dG-dC)·poly(dG-dC). Each point in the graph is an average of duplicate tests. Poly(dA-dT)·poly(dA-dT) and poly(dG-dC)·poly(dG-dC) were of the same length.

Binding of ADPRT to Bacteriophage T4 DNA. Bacteriophage T4 DNA (65.5% A+T) can be physiologically glucosylated with bulky glucose residues, resulting in a partial (31%) shielding of the major groove (Revel, 1983; Mirzabekov et al., 1977). Figure 7 illustrates that ADPRT does not bind to glucosylated T4 DNA (gluc 5-(hydroxymethyl)cytosine), whereas ADPRT readily associated with nonglucosylated T4 DNA (5-(hydroxymethyl)cytosine), further supporting the view that ADPRT makes major groove contacts, which are necessary for the binding of ADPRT to T4 DNA. Results of this experiment agree with the conclusions derived from the protection by ADPRT against methylation by DMS. The inherent differences in the binding assays (nitrocellulose filter binding vs DMS protection) and the differences in DNAs employed prohibit quantitative comparisons.

Binding of a 36-kDa Polypeptide of ADPRT to the 209-bp SV40 Fragment. Figure 8A (lane 5) illustrates that only a 36-kDa polypeptide binds strongly to the ^{32}P-labeled DNA fragment. Traces of other peptides, which are known to be precursors of the 36-kDa peptide (Buki & Kun, 1988), displaying only weak affinity for the ^{32}P-labeled DNA fragment, are also seen, but the 36-kDa polypeptide is the only major band. The 36-kDa band was previously shown (Buki & Kun, 1988) to be a doublet consisting of two polypeptides differing by one lysine residue. Only one polypeptide (peptide A) showed binding to the ^{32}P-labeled DNA fragment (lane 4, Figure 8B). Furthermore, it was found that binding of a polyclonal antibody (Buki & Kun, 1988) raised against the whole ADPRT protein did not prevent the binding of the ^{32}P-labeled DNA fragment to either the whole protein or to the DNA-binding 36-kDa A peptide (data not shown).

The 36-kDa Peptide Generates the Same DNase I Pattern as the Whole ADPRT Protein. The equivalency of the 36-kDa A polypeptide with ADPRT is illustrated in Figures 3–5 (see legends). The polynucleotide poly(dI-dC)·poly(dI-dC), by competing with the 209-bp fragment, also produces the same DNase I digestion pattern when ADPRT is replaced by the 36-kDa A (Figures 4 and 5, see legend).

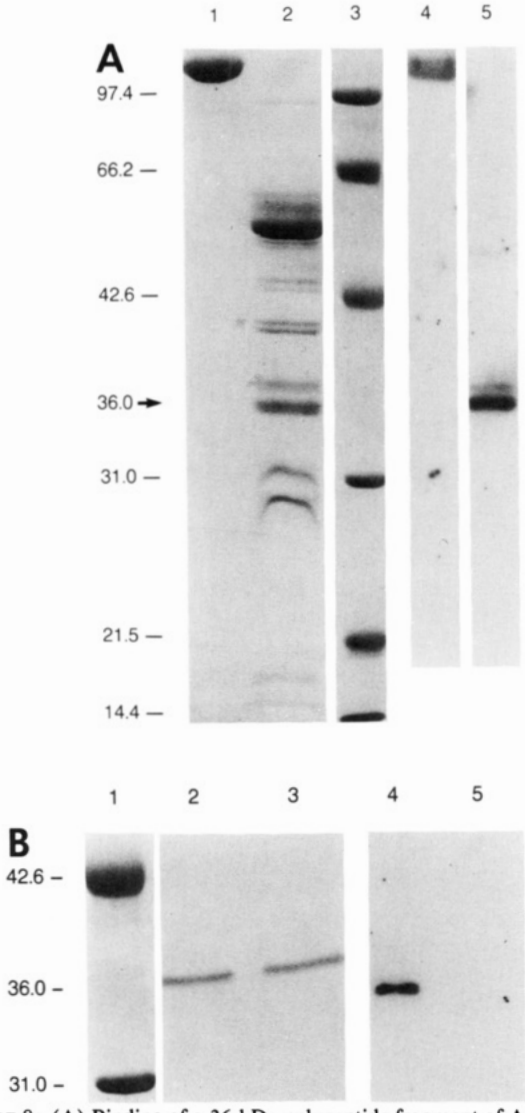

FIGURE 8: (A) Binding of a 36-kDa polypeptide fragment of ADPRT to the 209-bp *Eco*RI–*Pst*I SV40 DNA fragment ^{32}P-labeled at the 3′*Eco*RI site: Plasmin-digested ADPRT fragments were separated on an SDS–polyacrylamide gel as described earlier (Buki & Kun, 1988). When the DNA-binding assay was employed, the membrane containing the polypeptides was directly exposed to ^{32}P-labeled DNA. (Lane 1) Undigested ADPRT (immunostain using a polyclonal anti-ADPRT antibody); (lane 2) plasmin-digested ADPRT (transblot, immunostain); (lane 3) protein standards specified in kilodaltons on the left-hand side of the figure (Coomassie Brilliant Blue stain) (97.4 = phosphorylase B; 66.2 = bovine serum albumin; 42.6 = ovalbumin; 31.0 = carbonic anhydrase; 21.5 = soybean trypsin inhibitor; 14.4 = lysozyme) [purchased from Bio-Rad Co (Richmond, CA)]; (lane 4) undigested ADPRT bound to ^{32}P-labeled DNA (transblot); (lane 5) 36-kDa polypeptide bound to ^{32}P-labeled DNA (transblot). Lanes 4 and 5 are autoradiograms. Lanes 1 and 2 contained ~3 μg of protein per lane on the gel before electroblotting. Lane 3 contained ~1 μg of protein standards. (B) Binding of the 36-kDa polypeptide (A) to the 209-bp *Eco*RI–*Pst*I SV40 DNA fragment ^{32}P-labeled at the 3′*Eco*RI site: (lane 1) protein standards (42.6 = ovalbumin; 31.0 = carbonic anhydrase); (lane 2) 36-kDa polypeptide A (transblot, immunostain); (lane 3) 36-kDa polypeptide B (transblot, immunostain); (lane 4) 36-kDa polypeptide A bound to ^{32}P-labeled DNA (transblot); (lane 5) 36-kDa polypeptide B not bound to ^{32}P-labeled DNA (transblot). Lanes 2–5 contained ~2 μg of protein per lane on the gel before electroblotting. Lane 1 contained ~1 μg of protein. Lanes 2 and 3 were immunostained. Lanes 4 and 5 are autoradiograms. Only the relevant portions of the gel or the autoradiograms are shown.

The 209-bp EcoRI–PstI Fragment Is Intrinsically Bent. The reduced mobility of certain restriction fragments on high-percentage polyacrylamide (5–12% acrylamide) gels, as

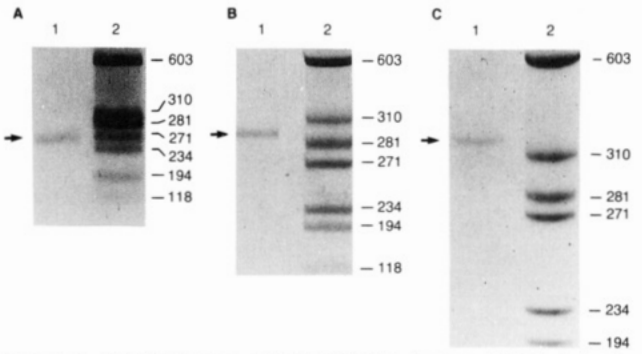

FIGURE 9: 209-bp *Eco*RI–*Pst*I SV40 DNA fragment is intrinsically bent: (A) 2% agarose gel; (B) 5% acrylamide gel; (C) 12% acrylamide gel. Lane 1 in each panel shows the 209-bp *Eco*RI–*Pst*I SV40 DNA fragment (arrows). Lane 2 in each panel shows bacteriophage φX174 replicative form DNA cut with *Hae*III, which served as markers. Lane 1 in each panel contained 5 ng (~2×10^3 cpm) of ^{32}P-labeled DNA fragment. Lane 2 in each panel contained 5 ng (~2×10^4 cpm) of nick-translated φX174 double-stranded DNA *Hae*III markers. Only the relevant portions of the gels are shown.

compared to the expected mobility, which is based on their known lengths, has been attributed to intrinsic DNA bending (Marini et al., 1982; Koo et al., 1986). DNA bending has been correlated to the presence of adenine–thymine tracts (Koo et al., 1986) and/or ApA wedges (Ulanovsky & Trifonov, 1987; Hagerman, 1986) that are present in the helical repeat of DNA.

Applying the accepted criteria of DNA bending (Koo et al., 1986; Ulanovsky & Trifonov, 1987), several loci of potential bending were found in the 209-bp *Eco*RI–*Pst*I fragment (Figure 10E; capitalized dAs). The presence of DNA bends was tested by the mobility-retardation assay on nondenaturing polyacrylamide gels. As illustrated in Figure 9A the 209-bp fragment migrated between the 271- and 281-bp markers on a 2% agarose gel, whereas on a 5% polyacrylamide gel it did so between the 281- and 310-bp markers (Figure 9B); on a 12% polyacrylamide gel, the 209-bp fragment migrated at approximately 350 bp (Figure 9C). That is, there was an overestimation of 167.4%, and the ratio of apparent length to the actual length at 4 °C is 1.674. Consistent with the behavior of bent DNA (Griffith et al., 1986; Levene et al., 1986), the 209-bp fragment migrated at approximately its expected size on a 4% polyacrylamide gel that was run at room temperature (22 °C) and at 75 V (data not shown). Recently Milton and Gesteland (1988) confirmed the presence of a DNA bend in a 752-bp restriction fragment of SV40 that included the 209-bp *Eco*RI–*Pst*I region.

Other DNA fragments of comparable size to the 209-bp DNA, such as the *Eco*RII G fragment, the *Acc*I–*Eco*RI of SV40 (Milton & Gesteland, 1988), and the *Bam*HI–*Sal*I of *pBR*322, which have no bent structures (data not shown), did not bind ADPRT in a manner that produced endonuclease protection. Although we have not rigorously demonstrated the requirement for a bent structure of DNA for ADPRT binding, the coincidence of ADPRT binding and the presence of bent structure(s) in the 209-bp SV40 DNA raises the need for further studies capable of testing the causality of static and induced bent structures and ADPRT binding mechanisms.

It has been suggested that oligo(dA·dT) regions of DNA are structures which favor DNA bending (Koo et al., 1986; Ulanovsky & Trifonov, 1987). Since the 209-bp DNA that binds ADPRT in the internal regions contains 60% dA+dT sequences, we tested synthetic poly(dA-dT)·poly(dA-dT) and poly(dG-dC)·poly(dG-dC) deoxyribonucleotides for ADPRT binding. As illustrated in Figure 7, poly(dA-dT)·poly(dA-dT)

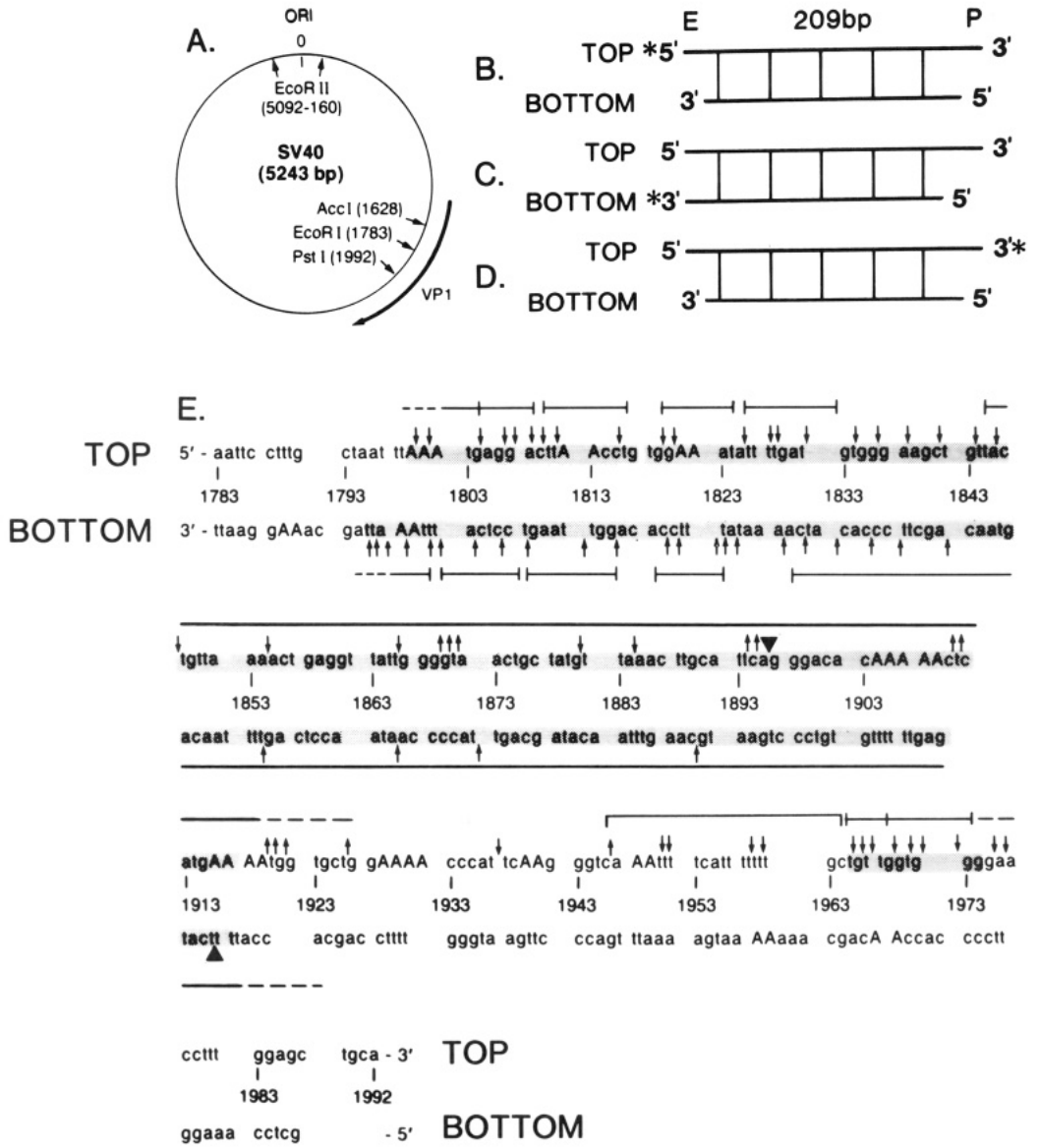

FIGURE 10: (A) Positions of the different fragments used in the present work and their restriction sites on the SV40 circular map. The circular SV40 map, with only the relevant SV40 landmarks, was drawn according to the method of Buchman et al. (1980). "Ori" is the origin of replication. The thick arrow shows the direction of transcription of the gene coding for VP1. (B–D) Schematic diagram of the 209-bp SV40 fragment showing the location of the ^{32}P end label (*). The top and bottom strands, and the *Eco*RI (E) and *Pst*I (P) sites, are also indicated. The vertical lines suggest the double-stranded nature of the DNA. (E) Nucleotide sequence of the 209-bp *Eco*RI–*Pst*I fragment of SV40 DNA and a summary of DNase I protection data. Arrows pointing inside (i.e., toward the DNA backbone) show examples of several sites of suppressed DNase I cleavage in the presence of ADPRT or the 36-kDa A polypeptide, whereas arrows pointing outside (i.e., away from the DNA backbone) show sites of enhanced DNase I cleavage. Each arrow does not always indicate the presence of only one band on the gel but may represent close multiple sites that have not been resolved. The brackets (⊢⊣) denote binding regions for ADPRT or the 36-kDa A polypeptide. The brackets are drawn in an arbitrary manner to show binding regions falling between the most prominent DNase I cutting sites. The hyphenated lines (— - - -) signify the lack of definition at the ends of the DNase I protected regions. ⌐¬ indicates a region where DNase I cutting was infrequent on naked DNA. ▲ and ▼ are λ *exo* pause sites in the presence of ADPRT. The shaded sequences signify overall protection by ADPRT against DNase I at the highest concentration of ADPRT. Capitalized dA tracts and ApA wedges indicate loci of potential bending.

binds at least twice as strongly as poly(dG-dC)·poly(dG-dC), consistent with the assumption that oligo(dA·dT) structures in bent DNA contribute to ADPRT binding capability.

It is interesting that in the 209-bp *Eco*RI–*Pst*I fragment prominent λ *exo* pause sites (~1950 and 1912, Figure 1A; ~1898, Figure 1B) and probable bending (capitalized dA tracts, Figure 10E) nearly coincide, suggesting that λ *exo* may detect bent structures.

Discussion

To our knowledge exonuclease protection experiments are the first direct demonstration of the binding of ADPRT to termini of DNA fragments, although this type of association has been implicated by indirect experiments consisting of the catalytic activation of ADPRT by nucleases (Benjamin & Gill, 1980a,b; Berger & Petzold, 1985). Earlier workers considered the binding of ADPRT to termini as the only catalytically meaningful ADPRT–DNA association, which is understandable since the DNA-condensing effect of ADPRT on closed circular DNA (Sastry & Kun, 1988) was unknown until recently. The effect of ADPRT on DNA conformation (Sastry & Kun, 1988) introduces complications in all experiments where enzymatic probes are being applied to detect ADPRT–DNA binding. The mode of action of λ exonuclease on the 209-bp SV40 DNA fragment (Figure 1) is also anomalous when ADPRT is bound to DNA. Changes in pause sites (Figure 1) and differences in protected regions between the two DNA strands upon ADPRT binding (Figures 3–5) appear

to indicate conformational alterations in DNA, which can secondarily modify the sites of attack by exo- and endonucleases. Our results are in disagreement with those of de Murcia et al. (1983), who reported that ADPRT does not associate significantly with DNA termini—a conclusion based solely on electron microscopy. The direct test of ADPRT binding to DNA termini by exonuclease protection avoids possible technical artifacts that may occur in electron microscopy. More importantly, the binding of ADPRT to termini of restricted DNAs is indiscriminate, whereas the binding of ADPRT to internal regions, as assayed by endonuclease protection, is not, and thus far only few DNAs, notably the 209-bp SV40 fragment, exhibit typical endonuclease protection by ADPRT. We have also observed protection by ADPRT against DNase I on a 237-bp *Bam*HI–*Bcl*I fragment (65.5% dA+dT; positions 2533–2770) of SV40 DNA (results not shown). This fragment has been shown to be bent (Milton & Gesteland, 1988). It is therefore proposed that binding sites of ADPRT to internal regions of restricted DNAs or binding of ADPRT to intact circular DNA may require certain structural features, DNA bending being one of them. Identification of these structures and participation of the second species of protein ligands, namely histones (Sastry & Kun, 1988), in ADPRT–DNA binding is the subject of further research. The more discriminating binding of ADPRT to internal regions of restricted DNA is also complicated by the ADPRT-induced structural changes in DNA that we recently reported (Sastry & Kun, 1988). Enhancement and inhibition of the enzymatic attack by DNase I on the 209-bp SV40 DNA (Figures 3–5) can only be rationalized if one considers structural alterations of DNA as a consequence of the binding of ADPRT. The association of ADPRT to internal regions of the 209-bp DNA fragment does not comply with the criteria set forth for the binding mechanisms of DNA sequence-specific proteins that leave distinct footprints. Therefore, ADPRT appears to be a protein that binds to certain relatively infrequent DNA structures and not sequences. Binding of ADPRT occurs along the major groove of the 209-bp SV40 DNA with apparent varying affinities along the internal regions of DNA, discriminating, however, between top and bottom DNA strands (see Materials and Methods). Our experimental model at best yields semiquantitative results, and the determination of various affinities between ADPRT and various DNA sequences requires a more quantitative experimental approach. Previous results (Sastry & Kun, 1988) already forecast different affinities between different fragments and ADPRT. On the basis of competition experiments with poly(dI-dC)-poly(dI-dC), which does not show endonuclease protection in the presence of ADPRT, we propose that the binding of ADPRT to the 209-bp fragment commences with association to DNA termini followed by subsequent binding to internal regions containing DNA bends. If a DNA does not contain structures that are able to bind ADPRT in its internal regions (e.g., *Bam*HI–*Sal*I fragment of *pBR*322), then only the indiscriminate binding to termini occurs.

Application of the 36-kDa polypeptide of ADPRT as the protective molecule against DNase I attack on the 209-bp SV40 DNA may simplify research aimed at the identification of the mechannsms of DNA–ADPRT binding. The identification of DNA bends as an essential feature of the binding regions of ADPRT to DNA requires further analysis. The biological role of DNA bends in gene regulation (Bossi & Smith, 1984; Zahn & Blattner, 1987; Ryder et al., 1986; Travers, 1987; Williams et al., 1988) is presently developing, and if this structure proves important in ADPRT–DNA interactions, the biological function of ADPRT may be better understood in molecular terms.

Acknowledgments

We thank Dr. Jerome McLick for helpful comments.

References

Althaus, F. R., & Richter, C. (1987) in *ADP-ribosylation of proteins*, pp 1–10, Springer-Verlag, New York.
Angle, P., Allegretto, E. A., Hattori, K., Boyle, W. J., Hunter, T., & Karin, M. (1988) *Nature (London) 332*, 166–171.
Benjamin, R. C., & Gill, D. M. (1980a) *J. Biol. Chem. 255*, 10502–10508.
Benjamin, R. C., & Gill, D. M. (1980b) *J. Biol. Chem. 255*, 10493–10501.
Berger, N. A., & Petzold, S. J. (1985) *Biochemistry 24*, 4352–4355.
Bossi, L., & Smith, D. M. (1984) *Cell 39*, 643–652.
Brenowitz, M., Senear, D. F., Shea, M. A., & Ackers, G. K. (1986) *Proc. Natl. Acad. Sci. U.S.A. 83*, 8462–8466.
Buchman, A. R., Burnett, L., & Berg, P. (1980) in *DNA Tumor Viruses* (Tooze, J., Ed.) pp 799–829, Cold Spring Harbor Laboratory, Cold Spring Harbor, NY.
Buki, K., & Kun, E. (1988) *Biochemistry 27*, 5990–5995.
Buki, K., Kirsten, E., & Kun, E. (1987) *Anal. Biochem. 167*, 160–166.
de Murcia, G., Jongstra-Bilen, J., Ittel, M. E., Mandel, P., & Delain, E. (1983) *EMBO J. 2*, 543–548.
Dynan, W. S., & Tjian, R. (1983) *Cell 32*, 669–680.
Dynan, W. S., Tjian, R., & Schimke, R. T. (1986) *Nature (London) 319*, 246–248.
Elbrecht, A., Tsai, S. Y., Tsai, M.-J., & O'Malley, B. W. (1985) *DNA 4*, 233–240.
Gaal, J. C., & Pearson, C. K. (1985) *Biochem. J. 230*, 1–18.
Galas, D. J., & Schmitz, A. (1978) *Nucleic Acids Res. 5*, 3157–3171.
Griffith, J., Bleyman, M., Rauch, C. A., Kitchin, P. A., & Englund, P. T. (1986) *Cell 46*, 717–724.
Hagerman, P. J. (1986) *Nature (London) 321*, 449–450.
Hochschild, A., Douhan, J., III, & Ptashne, M. (1986) *Cell 47*, 807–816.
Koo, H.-S., Wu, H-M., & Crothers, D. M. (1986) *Nature (London) 320*, 501–506.
Kun, E., Minaga, T., Kirsten, E., Jackowski, G., McLick, J., Peller, L., Oredsson, S. M., Marton, L., Pattabiraman, N., & Milo, G. (1983a) *Adv. Enzyme Regul. 21*, 177–201.
Levene, S. D., Wu, H.-M., & Crothers, D. M. (1986) *Biochemistry 25*, 3988–3995.
Lui, L. F., & Wang, J. C. (1978) *Cell 15*, 979–984.
Maniatis, T., Fritch, E., & Sambrook, J. (1982) *Molecular Cloning—A Laboratory Manual*, Cold Spring Harbor Laboratory, Cold Spring Harbor, NY.
Marini, J. C., Levene, S. D., Crothers, D. M., & Englund, P. T. (1982) *Proc. Natl. Acad. Sci. U.S.A. 79*, 7664–7668.
Maxam, A., & Gilbert, W. (1980) *Methods Enzymol. 65*, 499–560.
Milton, D. L., & Gesteland, R. F. (1988) *Nucleic Acids Res. 16*, 3931–3949.
Minaga, T., & Kun, E. (1983a) *J. Biol. Chem. 258*, 725–730.
Minaga, T., & Kun, E. (1983b) *J. Biol. Chem. 258*, 5726–5730.
Mirzabekov, A. D., San'ko, D. F., Kolchinsky, A. M., & Melnikova, A. F. (1977) *Eur. J. Biochem. 75*, 379–389.
Morrison, A., & Cozzarelli, N. R. (1981) *Proc. Natl. Acad. Sci. U.S.A. 78*, 1416–1420.
Noll, M. (1974) *Nucleic Acids Res. 1*, 1573–1578.

Revel, H. (1983) in *The Bacteriophage T4* (Mathews, C. K., Kutter, E. M., Mosig, G., & Berget, P., Eds) pp 156-165, American Society for Microbiology, Washington, DC.
Riley, D., & Wientraub, H. (1978) *Cell 13*, 281-293.
Roychaudhary, R., & Wu, R. (1980) *Methods Enzymol. 65*, 43-63.
Ryder, K., Vakalopoulou, E., Mertz, R., Mastrangelo, I., Hough, B., Tegtmeyer, P., & Fanning, E. (1986) *Cell 42*, 539-548.
Sastry, S. S., & Kun, E. (1988) *J. Biol. Chem. 263*, 1505-1512.
Shalloway, D., Klienberger, T., & Livingston, D. M. (1980) *Cell 20*, 411-422.
Siebenlist, U., & Gilbert, W. (1980) *Proc. Natl. Acad. Sci. U.S.A. 77*, 122-126.
Slater, E. P., Rabenau, O., Karin, M., Baxter, J. D., & Beato, M. (1985) *Mol. Cell. Biol. 5*, 2984-2992.
Suck, D., & Oefner, C. (1986) *Nature (London) 321*, 620-625.
Sutcliffe, J. G. (1979) *Cold Spring Harbor Symp. Quant. Biol. 43*, 77-90.
Travers, A. A. (1987) *Trends Biochem. Sci. 12*, 108-112.
Ueda, K., & Hayaishi, O. (1985) *Annu. Rev. Biochem. 54*, 73-100.
Ulanovsky, L. E., & Trifonov, E. N. (1987) *Nature (London) 326*, 720-722.
Von der Ahe, D., Janich, S., Cheidereit, C., Renkawitz, R., Schutz, G., & Beato, M. (1984) *Nature (London) 313*, 706-709.
Williams, J. S., Eckdahl, T. T., & Anderson, J. N. (1988) *Mol. Cell. Biol. 8*, 2763-2769.
Wu, C. (1985) *Nature (London) 317*, 84-87.
Zahn, K., & Blattner, F. R. (1987) *Science 236*, 416-422.

Purification and Characterization of an Altered Topoisomerase II from a Drug-Resistant Chinese Hamster Ovary Cell Line†

Daniel M. Sullivan,‡ Michael D. Latham,‡ Tom C. Rowe,§ and Warren E. Ross*,‡

James Graham Brown Cancer Center, University of Louisville, Louisville, Kentucky 40292, and Department of Pharmacology and Therapeutics, University of Florida, Gainesville, Florida 32610

Received March 3, 1989

ABSTRACT: The cytotoxicity and DNA damage induced by the epipodophyllotoxins and several intercalating agents appear to be mediated by DNA topoisomerase II. We have purified topoisomerase II to homogeneity both from an epipodophyllotoxin-resistant Chinese hamster ovary cell line, Vpm^R-5, and from the wild-type parental cell line. Immunoblots demonstrate similar topoisomerase II content in these two cell lines. The purified enzymes are dissimilar in that DNA cleavage by Vpm^R-5 topoisomerase II is not stimulated by VP-16 or *m*-AMSA. Furthermore, the Vpm^R-5 enzyme is unstable at 37 °C. Thus, the drug resistance of Vpm^R-5 cells appears to result from the presence of an altered topoisomerase II in these cells. Purified topoisomerase II from VPM^R-5 and wild-type cells has the same monomeric molecular mass as well as equivalent catalytic activity with respect to decatenation of kinetoplast DNA. Etoposide (VP-16) inhibits the activity of both enzymes. Noncovalent DNA–enzyme complex formation, assayed by nitrocellulose filter binding, is also similar, as is protection from salt dissociation of this complex by ATP and VP-16. The data suggest a model in which the drug-resistant cell line, Vpm^R-5, has religation activity which is less affected by drug than that of the wild-type cells. Drug effect on DNA religation and catalytic activity are dissociated mechanistically. In addition, under certain circumstances, the "cleavable complex" observed following denaturation of a drug-stabilized DNA–enzyme complex may not adequately reflect the nature of the antecedent lesion. As the first mammalian cell line bearing an altered topoisomerase II, this line will provide a useful system for further examination of the actions of topoisomerase II.

DNA type II topoisomerases (EC 5.99.1.3) allow the interconversion of DNA topoisomers by introducing a transient enzyme-bridged double-strand DNA break. This reaction is thought to consist of five phases: (i) recognition and binding of the enzyme to its DNA substrate; (ii) double-stranded cleavage of DNA, forming a covalent phosphotyrosyl bond at the 5′ end of each strand; (iii) passage of a second DNA duplex through the break; (iv) religation of the DNA; and (v) the ATP-dependent turnover of topoisomerase II. Further details of this reaction mechanism and the role of such an enzyme in cellular processes have recently been reviewed (Wang, 1985; Vosberg, 1985; Maxwell & Gellert, 1986).

In addition to its enzymatic function(s) in normal cellular processes, recent evidence suggests that topoisomerase II is an intracellular target for several antineoplastic agents, specifically, the epipodophyllotoxins and intercalating drugs (Ross et al., 1984; Chen et al., 1984; Tewey et al., 1984a; Ross, 1985). These drugs allow topoisomerase binding and cleavage of DNA to proceed as outlined above but appear to block the religation step. This is manifested as increased DNA scission when the DNA–enzyme complex is denatured. Although a general correlation between drug-induced DNA strand break frequency and cytotoxicity exists, definitive evidence for a

† This work was supported by USPHS Grants CA-24586 and CA-01124.
‡ University of Louisville.
§ University of Florida.

0006-2960/89/0428-5680$01.50/0